Journal Pre-proofs

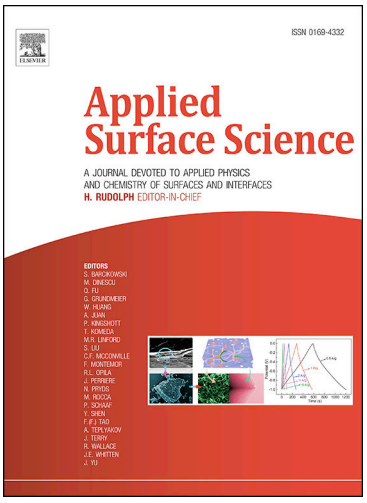

Full Length Article

Low-energy electron emission at the separation of gold-platinum surfaces induced by galactic cosmic rays on board LISA Pathfinder

Mattia Villani, Simone Benella, Michele Fabi, Catia Grimani

PII: S0169-4332(20)30490-6
DOI: https://doi.org/10.1016/j.apsusc.2020.145734
Reference: APSUSC 145734

To appear in: *Applied Surface Science*

Received Date: 7 October 2019
Revised Date: 4 February 2020
Accepted Date: 10 February 2020

Please cite this article as: M. Villani, S. Benella, M. Fabi, C. Grimani, Low-energy electron emission at the separation of gold-platinum surfaces induced by galactic cosmic rays on board LISA Pathfinder, *Applied Surface Science* (2020), doi: https://doi.org/10.1016/j.apsusc.2020.145734

Low-energy electron emission at the separation of gold-platinum surfaces induced by galactic cosmic rays on board LISA Pathfinder

Mattia Villani*

DiSPeA, University of Urbino "Carlo Bo", Urbino, Italy

National Institute for Nuclear Physics , Florence, Italy

Simone Benella

DiSPeA, University of Urbino "Carlo Bo", Urbino, Italy

National Institute for Nuclear Physics , Florence, Italy

Michele Fabi

DiSPeA, University of Urbino "Carlo Bo", Urbino, Italy

National Institute for Nuclear Physics , Florence, Italy

Catia Grimani

DiSPeA, University of Urbino "Carlo Bo", Urbino, Italy

National Institute for Nuclear Physics , Florence, Italy

Abstract

Galactic cosmic rays and solar energetic particles will induce spurious Coulomb forces on free-falling, gold-platinum test-masses on board the future interferometers for low-frequency gravitational wave detection in space. The European Space Agency mission LISA Pathfinder (LPF) was aimed to test the performance of instruments that will be placed on board LISA (Laser Interferometric Space Antenna), expected to be launched in 2034. Free-falling test-mass charging was measured on board LPF in 2016-2017. Simulations of this charging process were carried out before the mission launch with GEANT4 and Fluka Monte Carlo tools. A very good agreement was found between net charging measurements and simulations, while the shot noise, associated with the charging process, resulted 3-4 times larger than expected. New dedicated simulations aiming to study in detail the low-energy electron emission from metal electrodes surrounding the test-masses reveal that the mismatch between measurements and former simulations may be due to the lack of propagation of electrons with

*Corresponding author

Email address: mattia.villani@uniurb.it (Mattia Villani)

energies smaller than the average ionization potential in the Monte Carlo tools mentioned above. Preliminary results are presented and discussed here.

Keywords: Instrumentation: Interferometers; Cosmic-ray interactions

1. Introduction

LISA Pathfinder (LPF) [1, 2, 3, 4] was a space mission dedicated to the test of the technology that will be placed on board LISA, the space-borne interferometer of the European Space Agency aiming to the detection of low-frequency gravitational waves (GWs) between 10^{-4} and 10^{-1} Hz [5].

The LPF spacecraft (S/C) was launched with a Vega rocket from the Kourou base in French Guiana on December 3, 2015 and reached its final orbit, around the first Lagrangian point L1 at 1.5 million km from Earth in the Earth-Sun direction, by the end of January 2016. The heart of the LPF satellite is a system of two 2-kg test-masses (TMs), made of a gold-platinum alloy which play the role of mirrors of the on-board interferometer. A system of electrodes allows for the actuation and position measurement of the TMs that must nominally remain in free fall, centered within the electrode housing. LPF proved that the technology for space-borne GW detectors is mature for having measured a residual spurious acceleration of the TMs of the order of femto-g, by exceeding the most optimistic expectations [4]. The mission ended on July 18, 2017.

One of the major concerns before the mission launch was to correctly estimate the low-frequency acceleration noise due to the charges deposited in the TMs by galactic cosmic rays (GCRs) and solar energetic particle (SEP) interactions. Particles from keV to GeV energies are accelerated in the inner heliosphere by shocks produced by coronal mass ejections and in solar flares. No SEP event characterized by an overall particle flux larger than the GCR background occurred during the period LPF remained in orbit. Consequently, it was possible to study only the role of GCRs with energies exceeding 100 MeV n^{-1} penetrating the spacecraft material (about 13 g cm^{-2}) and charging the TMs. Predictions of GCR fluxes were carried out to estimate the net and effective TM charging for the time period the mission was supposed to be orbiting around L1 [6, 7, 8, 9]. The net charging simulations resulted in agreement with observations, while the effective charging (charging shot noise) was underestimated by a factor 3-4 [10]. The optimum agreement between net charging and observations indicated that the simulations benefited of good predictions of the GCR fluxes while, the high experimental values of the shot noise compared to simulations, seemed to suggest that seldom only a large number of particles were released in the TMs by affecting the shot noise but leaving the net charging basically unchanged. The most plausible Monte Carlo simulation limitations were ascribable to the lack of proper electron propagation down to about 10 eV in metals in Monte Carlo tools GEANT4 [11] and Fluka [12, 13]. Ten eV electrons have mean free paths of approximately 10 Å in gold and do not show yet quantum mechanical behavior. The propagation of such low-energy electrons is often

neglected, since it increases enormously the simulation time while, in general, does not affect the results[1]. However, this approach was not appropriate in the case of LPF that allowed to monitor the electron production at the separation of gold-platinum surfaces induced by GCRs for the first time.

A dedicated *Low-Energy Ionization* (LEI)[2] Monte Carlo was developed. The first version was written in Wolfram Mathematica, but the execution time was not optimal, since, for instance, computing time of a few hours was needed to simulate incident protons. The Python language did not allow for better results, therefore a new version of the program was written in Fortran 95. This last version takes about 20 minutes for the proton simulations. Further improvements may be considered in the future especially for incident nuclei that require computing times larger than for protons.

This paper is organized as follows: in Section 2 the pre-launch LPF TM charging simulations are reported; in Section 3 the LEI Monte Carlo program is illustrated and in section 4 results are presented and discussed.

2. LPF test-mass net and effective charging

The net charge deposited in the LPF TMs (λ_{net}) and the shot noise associated with the effective charging (λ_{eff}) are defined as follows (see [9]):

$$\lambda_{net} = \sum_{j_{net}=-\infty}^{+\infty} j_{net}\lambda_{j_{net}} \qquad \lambda_{eff} = \sum_{j_{eff}=-\infty}^{+\infty} (j_{eff})^2\lambda_{j_{eff}} \tag{1}$$

where j_{net} is the net charge deposited by each cosmic ray particle interaction calculated by algebraically summing up the contribution of positive and negative charges and j_{eff} is the effective charge deposited in terms of equivalent single charges by summing up the contribution of both positive and negative charges. $\lambda_{j_{net}}$ and $\lambda_{j_{eff}}$ are the occurrence rate of the associated deposited charge. Please note that λ_{net} and λ_{eff} in eqn. (1) have the same meaning than in eqns. (10) and (11) in [9]. In this work we have chosen to adopt different symbols for j_{net} and j_{eff} for helping the reader instead of explaining the difference in the text only as it was done in ref. [9].

The measured TM charging at the beginning of the mission is reported in table 1 [10]. The simulations described in [6, 7, 8, 9] carried out with protons and helium nuclei as incident particles predicted a net charge ranging between 15 and 33 e^+ s^{-1}, in line with the measured values, while for the effective charging the simulations predicted a value around 300/400 e s^{-1}, about a factor 3-4 below the measured value.

[1] Recently, after the publication of the papers [6, 7, 8, 9], the PENELOPE models for GEANT4 were released [11]. The PENELOPE models allow for the propagation of electrons with energies above 65 eV. This is an important improvement, but still insufficient for the LPF application we are dealing with in this work.

[2] The LEI program can be downloaded from `https://pasme.uniurb.it/`.

	Test Mass 1	Test Mass 2	
λ_{net}	$+22.9$	$+24.5$	$e^+ s^{-1}$
λ_{eff}	1060 ± 90	1360 ± 130	$e\ s^{-1}$

Table 1: Net and effective charging of LPF TMs measured on April 20-23, 2016 [10].

In order to investigate the origin of this mismatch, the dedicated LEI Monte Carlo program was developed as illustrated in the next section.

3. The *LEI* Monte Carlo program

To our knowledge, no Monte Carlo tool allowing for the propagation of low-energy electrons (down to eV scale) generated by the interaction of high-energy ions in metals is publicly available.[3] The LEI Monte Carlo program was written to provide the number, n, of electrons with kinetic energy E emitted at the separation of metal surfaces on the basis of the differential flux parameterized by Cucinotta et al. [15] for incoming ions:

$$\frac{dn}{dE} = \frac{2\pi N e^4}{mc^2\beta^2}\frac{Z_s^2}{E^2}\left[1 - \frac{\beta^2 E}{E_m} + \frac{\pi\beta Z_s^2}{137}\sqrt{\frac{E}{E_m}}\left(1 - \frac{E}{E_m}\right)\right] dx \tag{2}$$

where $\beta = v/c$ is the ion velocity, while:

$$E_m = \frac{2mc^2\beta}{1-\beta^2} \tag{3}$$

is the maximum kinetic energy that can be transferred to a single electron, N is the electron density of the material and dx its thickness; m and e are electron mass and charge, respectively, and finally

$$Z_s = Z\left[1 - \exp\left(-\frac{125\beta}{Z^{2/3}}\right)\right] \tag{4}$$

is the effective charge of nuclei with atomic number Z (not to be confused with the effective charging). The energy spectra of the simulated incident ions is generated by properly weighting the GCR flux interpolated with the function:

$$f(E) = A(E+b)^{-\alpha}E^{\beta} \quad \text{Particles m}^{-2}\text{s}^{-1}\text{sr}^{1}\text{GeV}^{-1}$$

in the range 0.1-200 GeV (see [16] for details). For the LPF mission beginning, when the effective charging was measured, the parameters A, b, α and β are

[3] The program TRAX [14] allows for the propagation of low-energy electrons, but the energy of the primaries is limited to 100 MeV while the GCR energy is several orders of magnitude higher.

Nucleus	A	b	α	β
p	18000	1.19	3.66	0.87
He	850	0.96	3.23	0.48
C	23	0.99	3.10	0.35

Table 2: Parameter values of the energy spectra interpolations adopted in this work [9, 16].

indicated in table 2 for protons (p), helium (He) and carbon (C) nuclei. Nitrogen, oxygen, neon, magnesium, silicon and iron nuclei were also considered in the simulations. The energy differential fluxes of these nuclei were obtained by considering the same parameters b, α and β used for carbon while to the parameter A the values 5.9, 21, 3.4, 4.2, 2.9, and 1.9, respectively, were assigned [16]. GCR particle initial positions and angle of incidence were randomly generated on a sphere surrounding the external surface of the electrodes in order to save computing time, since LEI allows for the propagation of ions with a step length of 1 nm and of electrons with a step length of 1 Å. At each step, the energy deposited in the material is subtracted from the ion energy. The energy of each produced electron is also subtracted from the incoming ion energy. The electron energy is generated as indicated in eqn. (2). The electron direction is assigned on the basis of the following eqn. (5) according to Cucinotta et al. [15]:

$$\cos\theta = \sqrt{\frac{E}{E_m}} \tag{5}$$

where θ is the escaping electron direction with respect to the incident ion direction. Electrons are propagated until leaving the electrodes or stopping in the material. The minimum energy of the produced electrons was set to 10 eV to limit the simulation time and to avoid quantum mechanics effects. Only the geometry of the LPF TM housing was implemented in LEI (see figure 1).

4. Low-energy electron emission at gold-platinum electrode-TM surface separation

Incident particles were impinging on the 0.9 μm Ti+Au electrode coating surrounding the TMs. Due to the nanometer to angstrom range of very low-energy electrons, these particles escape the electrode surface only if produced at the very edge of the material layer.

For each ion species, two simulations were performed in order to disentangle the role of the primary and secondary ionizations. By considering only the primary ionization (second column of table 3), a few hundreds of low-energy electrons were emitted at the electrodes surface and were deposited in the TMs. The dominant effect contributing to the effective TM charging is given by the secondary ionization that increases the number of emitted electrons by about a factor of 5 (see third column of table 3). The overcoming role of the secondary ionization was expected (see for example [17]).

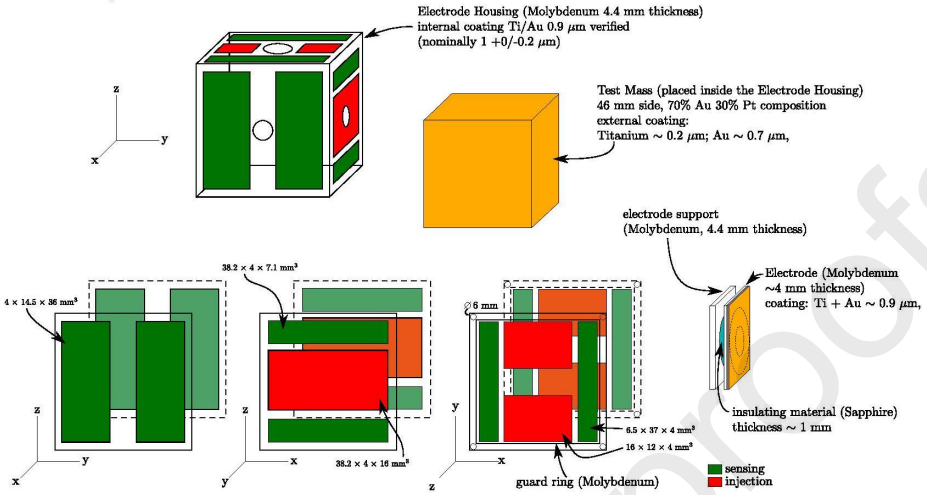

Figure 1: Geometry of the LPF electrode housing. In yellow the cubic TM made of gold with side of 4.6 cm is presented. The TM is enclosed into the TM housing which contains the electrodes (in red and green) of 0.9 μm thickness. A gap of 3 mm is present between the TM and the electrodes.

Ion	Primary ion. (e^- s^-)	Primary + secondary ion. (e^- s^{-1})	Percentage of interacting ions	Attenuated flux (e^- s^{-1})
p	79	612	7.5%	566
He	165	457	19.5%	368
C	9	212	28.5%	162
N	1	24	31.0%	17
O	4	133	32.5%	90
Ne	2	44	34.0%	29
Mg	36	192	35.5%	124
Si	6	30	39.0%	18
Fe	36	39	50.5%	18
TOTAL	341	1740		1392

Table 3: In the first column the ion species considered for the LEI simulations are indicated. In the second and third columns are reported the number of electrons deposited in the LPF TMs, produced by primary ionization and by primary and secondary ionizations. In the fourth column the percentage of interacting nuclei in the S/C is reported, while in the fifth column the number of electrons produced after the attenuation of incident particle fluxes is shown.

The results of the simulations described above constitute an approximate estimate of the low-energy electrons deposited in the TMs, because nuclei and target fragmentation, ionization energy losses and hadronic interactions in the material surrounding the TMs were not considered. The particle flux attenuation due to the passage of particles through the material surrounding the TMs was calculated on the basis of the cross section for nucleus-nucleus interactions

given by Westfall in [18] for energies > 10 GeV n^{-1}. Results are reported in column four of table 3. In the fifth column of the same table the number of the electrons produced after the ion flux attenuation is indicated. By comparing the fifth column of table 3 with the measurements reported in table 1, it can be observed that, by considering a conservative uncertainty of 30% affecting these simulations, that the low-energy electron charging of the TMs after the flux attenuation appears in good agreement with the measured one. The overall uncertainty was estimated as follows: a typical 10% uncertainty must be considered for the incident GCR fluxes as it was shown in [19] where the GCR proton integral flux prediction for the LPF mission beginning was found about 10% lower when compared to contemporaneous, analogous measurement of the AMS-02 experiment. Another contribution to the result uncertainty comes from the adopted Westfall cross section [18] which overestimates the attenuation of the incident flux at low energies (about half of the incident particles) by a factor of 2. The lack of particle ionization energy losses in the material surrounding the electrodes partly compensates the overestimated flux attenuation at low energies due to the use of the Westfall cross section [18]. For instance, Monte Carlo simulations show that protons below 200 MeV/n and heavy nuclei below 600 MeV/n do not reach the TMs due to ionization energy losses in the LPF S/C. This amount to a few percent of protons and about 25% of the nuclei sample. In order to better constrain our results, an upper limit to the low-energy electron charging due to protons incident on the TMs was set on the basis of a preliminary simulation where incoming particles were propagated with Fluka through 13 g cm^{-2} of aluminum (about the same grammage of the LPF satellite) before entering the TMs; the most abundant particle species (electrons, positrons at energies > 1 keV and pions) were propagated using LEI through the electrodes surrounding the TMs. The results of these simulations are considered an upper limit for low-energy electron emission, because hadronic interactions are characterized by a large transverse momentum and therefore in a wide geometry a smaller number of particles is supposed to reach the electrodes surrounding the TMs with respect to adopting a compact material arrangement. It was found that secondary charged particles are produced in a comparable number of the incoming protons thus producing an additional large number of low-energy electrons, that increases by 33% the charging induced by primary protons. This estimate was carried out by tracing with Fluka every particle entering and escaping the aluminum slab. Escaping particles were used as input data for the LEI program.

5. Conclusions

The LPF TM effective charging measurements revealed that the experimental results were severely under-estimated by Monte Carlo simulations. In this work we have explored the possibility that the lack of propagation of low-energy electrons in the material surrounding the TMs in Monte Carlo simulations might be responsible for the mismatch between estimates and observations. New simulations were carried out by using the dedicated program LEI which allows for the

propagation of low-energy electrons down to 10 eV. For a future more accurate work, we aim to implement the full LPF S/C geometry native in Fluka. GCR flux normalized on the basis of observations will be used in the simulations. Primary and secondary particles reaching the electrodes surrounding the TMs will be used as input data for LEI. The same will be done for particle escaping the TMs. The low-energy electron component estimated with LEI will be added to the Fluka simulations in both net and effective charging calculations.

Acknowledgment

The authors wish to thank Prof. E. Scifoni of the Trento Institute for Fundamental Physics and Application (TIFPA), Trento (Italy) for useful discussions.

References

[1] F.Antonucci *et al.*, Class. Quant. Grav. **28** 9 (2011) 094001;

[2] F.Antonucci *et al.*, Class. Quant. Grav. **29** 12 (2012) 124014;

[3] M.Armano *et al.* Phys. Rev. Lett. **116** 23 (2016), 231101;

[4] M. Armano *et al.*, Phys. Rev. Lett. **120** 6 (2018) 061101;

[5] P. Amaro-Seoane *et al.*, arXiv:1702.00786 [astro-ph.IM];

[6] P.Wass *et al.*, Class. Quant. Grav. **22** (2005) S311-S317;

[7] H.M. Araújo *et al.*, Astropart.Phys. **22** (2005) 451;

[8] C.Grimani *et al.*, Class. Quant. Grav. **22** (2005) S327-S332;

[9] C.Grimani *et al.*, Class. Quantum Grav. **32** (2015) 035001;

[10] M.Armano *et al.* Phys. Rev. Lett. **118.17** (2017) 171101;

[11] J.Allison *et al.*, Nucl. Instr. Meth. Phys. Res. A **835** (2016) 186;

[12] T.T. Böhlen, *et al.* Nuclear Data Sheets **120** (2014) 211;

[13] A. Ferrari, *et al.* CERN-2005-10 (2005), INFN/TC-05/11 SLAC-R-773;

[14] Krämer, M. and Kraft, G. Radiat. Environ. Biophys. **33** (1994) 91;

[15] F.A.Cucinotta *et al.*, AIP Conference Proceedings **362** (1996) 245;

[16] M.Armano, *et al.*, Ap.J. **854** (2018) 113;

[17] D.H. Perkins *Introduction to High Energy Physics* The Benjamin/Cummings Publishing Company, Inc. Printed in the United States of America, 1982.

[18] G.D. Westfall, *Phys. Rev. C* **19** (1979) 1309;

[19] C. Grimani, *et al.*, *Atmosphere* **10** (2019) 749.

- LISA PathFinders test mass effective charging
- Galactic Cosmic Ray interaction
- Low energy electrons

Conceptualization: Catia Grimani
Software: Mattia Villani, Michele Fabi
Writing original draft: Mattia Villani, Catia Grimani
Writing rewie and editing: Mattia Villani, Catia Grimani
Supervision: Catia Grimani
Project administration: Catia Grimani
Funding acquisition: Catia Grimani
Investigation: Mattia Villani
Validation: Simone Benella
Formal analysis:
Resources:
Data curation: Mattia Villani, Michele Fabi
Visualization

Declaration of interests

X The authors declare that they have no known competing financial interests or personal relationships that could have appeared to influence the work reported in this paper.

☐The authors declare the following financial interests/personal relationships which may be considered as potential competing interests: